Ionic Diodes

DOI: 10.1002/ange.201405755

Metastable Ionic Diodes Derived from an Amine-Based Polymer of Intrinsic Microporosity**

Elena Madrid, Yuanyang Rong, Mariolino Carta, Neil B. McKeown, Richard Malpass-Evans, Gary A. Attard, Tomos J. Clarke, Stuart H. Taylor, Yi-Tao Long, and Frank Marken**

Abstract: *A highly rigid amine-based polymer of intrinsic microporosity (PIM), prepared by a polymerization reaction involving the formation of Tröger's base, is demonstrated to act as an ionic diode with electrolyte-dependent bistable switchable states.*

Ionic diodes are analogous to the ubiquitous electronic diode and provide current rectification by the controlled transport of cations and anions instead of holes and electrons.[1] Such devices were first predicted and realized in the 1950s using the hindered mobility in cationic or anionic polymers or through a dialysis membrane.[2–4] This work was expanded into chaotic-ion-flux phenomena,[5] the first ionic transistor,[6] and further ionic rectification systems.[7–11] However, the potential importance of ionic diodes was recognized recently with the advent of nanofluidic devices and DNA-sequencing applications in biological nanopores.[12] To date, the fabrication of efficient ionic diodes involves a combination of hydrogel materials and/or complex nanofabrication processes with the use of composite materials and their methods of operation are not always fully understood. Hence, there is a requirement for ionic diodes to be prepared by simple fabrication techniques using a single well-defined material.

Polymers of intrinsic microporosity (PIMs) are composed of highly rigid and contorted macromolecules that preclude efficient packing to generate interconnected free volume.[13–15] They have been investigated for gas storage,[16] gas separations,[17–19] and as the active component for optical gas sensors.[20] Recently, a novel type of PIM was reported based on the polymerization of rigid aromatic diamine monomers using a reaction based on the formation of Tröger's base (TB).[13] For example, TB polymerization of diaminoethanoanthracene provides a highly rigid PIM (PIM-EA-TB; BET surface area ca. $1000\ m^2 g^{-1}$) with enhanced microporosity and exceptional potential as a gas separation membrane. Although most studies of PIM have focused on the selective transport of gases or vapors, PIM-EA-TB has recently demonstrated potential also as a membrane for electrocatalysis in which the transport of anions and cations is facilitated by the polymer's microporosity.[21,22] Here we describe a readily fabricated ionic diode based on PIM-EA-TB that demonstrates remarkable current rectification effects and allows the controlled transport of cations and anions by simple manipulation of the electrolyte properties.

Ionic diode fabrication was achieved by solution-casting a thin coating of PIM-EA-TB onto a 6 μm thick poly(ethylene terephthalate) (PET) film through which a single macropore was drilled by laser irradiation (≈ 4 μm diameter, Figure 1 A). The PET film was then placed into a two-compartment voltammetry cell (Figure 1 B) in contact with different electrolyte solutions on each face of the film and a potential applied across the PIM membrane to measure ion flow.

Cyclic voltammetry and impedance experiments were performed to assess ion transport in the PIM-EA-TB (Figure 2). Open circuit impedance characteristics were in agreement with a simple equivalent circuit based on 1) solution resistance R_S, 2) membrane capacitance C, and 3) macropore resistance R_P (see Figure 2 B). Whereas the membrane capacitance ($C = 0.8$ nF) and the solution resistance ($R_S =$ 600 Ω for 1 M NaCl based electrolyte) provide cell-parameters, the resistance R_P describes the macropore resistance due to restricted ion flow.

A PET film without pore resulted in insignificant current responses. With a pore, but in the absence of the PIM coating, the pore resistance is consistent with the electrolyte resistance within the macropore [Eq. (1)].

$$R_P^0 = \frac{1}{\Lambda_m^0}\frac{L}{A} = \frac{1}{u_+F + u_-F}\frac{L}{A} = 38\ k\Omega \qquad (1)$$

In this equation the limiting molar conductivity Λ_m^0, which is obtained from the ionic mobilities u_+ and u_- for Na^+ and Cl^- in water,[23] the pore length L and the macropore cross-sectional area A, allows the empty macropore resistance to be estimated to be 38 kΩ. In the presence of PIM-EA-TB in the macropore the resistance is increased by an order of magnitude and becomes characteristically pH-dependent (see Figure 2 B). Below a pH of 5 a significant decrease in R_P is indicative of 1) increased open-circuit mobility of ions

[*] Dr. E. Madrid, Y. Rong, Prof. F. Marken
Department of Chemistry, University of Bath
Claverton Down, Bath, BA2 7AY (UK)
E-mail: f.marken@bath.ac.uk
Dr. M. Carta, Prof. N. B. McKeown
School of Chemistry, University of Edinburgh
West Mains Road, Edinburgh, EH9 3JJ (UK)
E-mail: neil.mckeown@ed.ac.uk
R. Malpass-Evans, Prof. G. A. Attard, T. J. Clarke, Prof. S. H. Taylor
School of Chemistry, Cardiff University
Cardiff CF10 3AT (UK)
Prof. Y.-T. Long
Shanghai Key Lab of Functional Materials Chemistry & Department of Chemistry, East China University of Science and Technology
Shanghai 200237 (P. R. China)

[**] E.M. and F.M. acknowledge financial support from the EPSRC (EP/K004956/1). Y.R. thanks the University of Bath for a fee waiver.

Supporting information for this article is available on the WWW under http://dx.doi.org/10.1002/anie.201405755.

 © 2014 Wiley-VCH Verlag GmbH & Co. KGaA, Weinheim

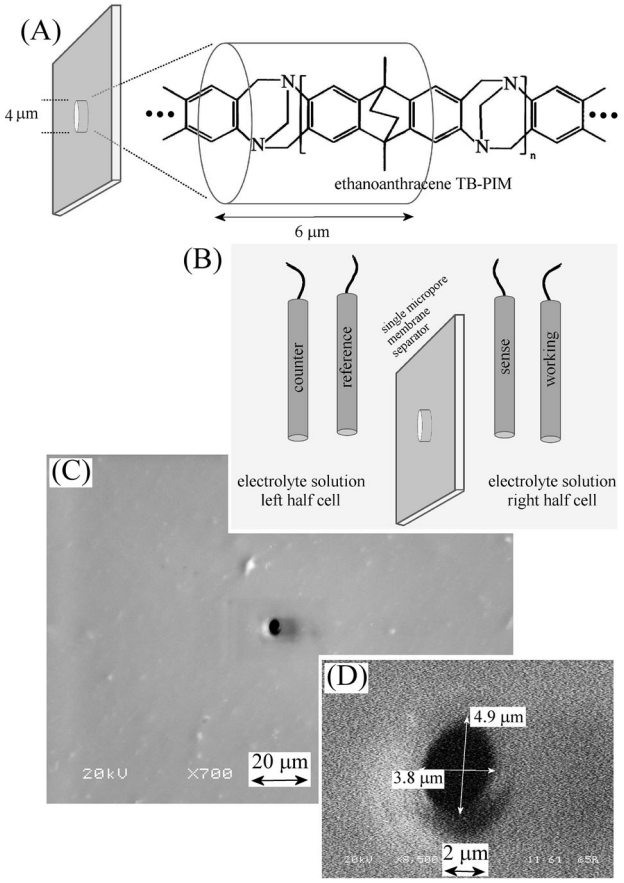

Figure 1. A) The molecular structure of PIM-EA-TB and B) the electrochemical cell with left and right half-cells filled with electrolyte. C, D) Scanning electron micrograph of the PET membrane (6 μm thickness) with a single pore (ca. 4 μm diameter) laser-machined into the center.

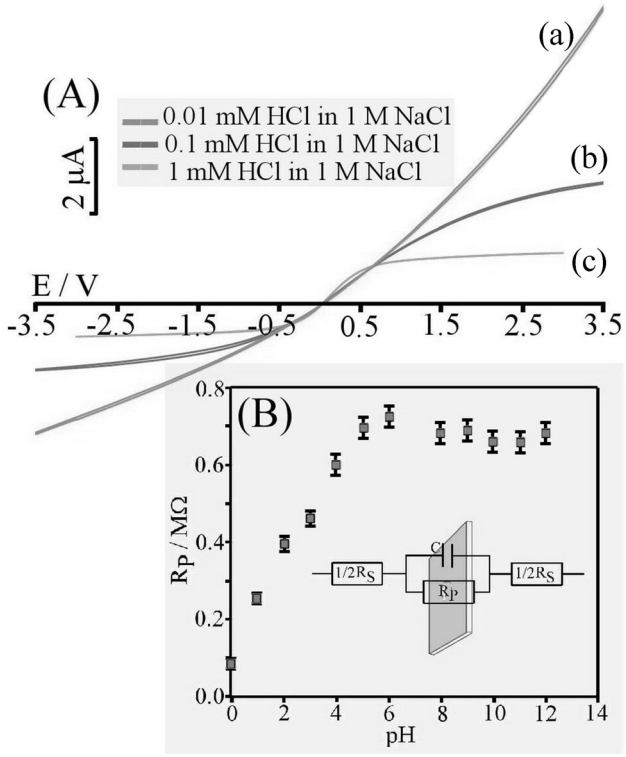

Figure 2. A) Cyclic voltammograms (scan rate 0.02 $V s^{-1}$) for the PIM-filled pore immersed in aqueous (a) 0.01, (b) 0.1, and (c) 1 mM HCl in 1 M NaCl. B) Equivalent circuit employed for impedance data analysis (at 0.0 V vs. SCE) and plot of R_P (fitting error below 1%; error bars estimated) at open circuit potential versus pH.

(e.g. protons) and 2) the onset of swelling (which has been reported previously to affect the transport in this PIM[21]) and which is consistent with BET pore data analysis for NaOH and HCl treated PIM-EA-TB (see Figure SI1).

Voltammograms recorded under the same experimental conditions exhibit stable time-independent characteristics (independent of scan rate over a range of 0.01 to 0.2 $V s^{-1}$) with PIM membranes proving reusability several times without loss of performance (they can be soaked in ethanol overnight). The voltammograms in Figure 2 A demonstrate the polarization characteristics of the PIM membrane. In alkaline and weakly acidic solution "ohmic slopes" suggest that migration within the pore is prevalent and ion transport is potential-driven. Perhaps surprisingly, under slightly more acidic conditions a plateau effect suggests interfacial transfer or diffusion limitation rather than migration (ohmic) control (Figure 2 Aiii). The anticipated diffusion-limited current for chloride anions in water to a 4 μm diameter pore is approximately[24] $I_{diffusion} = 4nF \times D \times r \times c = 1.5\ \mu A$ in good agreement with the observed current at pH 3 (here $n = 1$ for the charge transported by Cl^-, F is the Faraday constant, $D = 2 \times 10^{-9}\ m^2 s^{-1}$ is the diffusion coefficient for chloride,[25] r is the macropore radius, and c is the concentration of chloride). At pH 3 the plateau current scales with the chloride concentration, confirming this assignment. The additional currents observed 1) under alkaline conditions and 2) in the pH range lower than 2 are likely to be associated with additional cation transport.

Having identified pH-dependent ion transport phenomena for aqueous NaCl electrolyte, symmetric and asymmetric cells (with different electrolyte solution composition in left and right half cells) were investigated. Figure 3 shows that with aqueous 10 mM NaOH present on both sides, a "potential-driven" current response is observed associated with ion flow (presumably with contributions from both Na^+ and OH^-, see Figure 3) across the pore channel. In contrast, with aqueous 10 mM HCl on both sides, a diffusion-limited flow of anions with lower current is observed (Figure 3). Due to isolated protonation sites of the PIM-EA-TB, cation transport is believed to be slow and chloride transport dominates in 10 mM HCl. Both, the currents for 10 mM NaOH and the currents for 10 mM HCl scale approximately linearly with concentration (see Figure SI2).

For the asymmetric case with 10 mM HCl (left) and 10 mM NaOH (right) solutions separated by the PIM-EA-TB membrane, a strong current rectification is observed with the system acting as an ionic diode with a dramatic change in current depending on polarization and presence of ions (Figure 4).[26,27] This behavior is consistent with a mechanism in which there is combined flux of Na^+ and Cl^- in the "open"

© 2014 Wiley-VCH Verlag GmbH & Co. KGaA, Weinheim

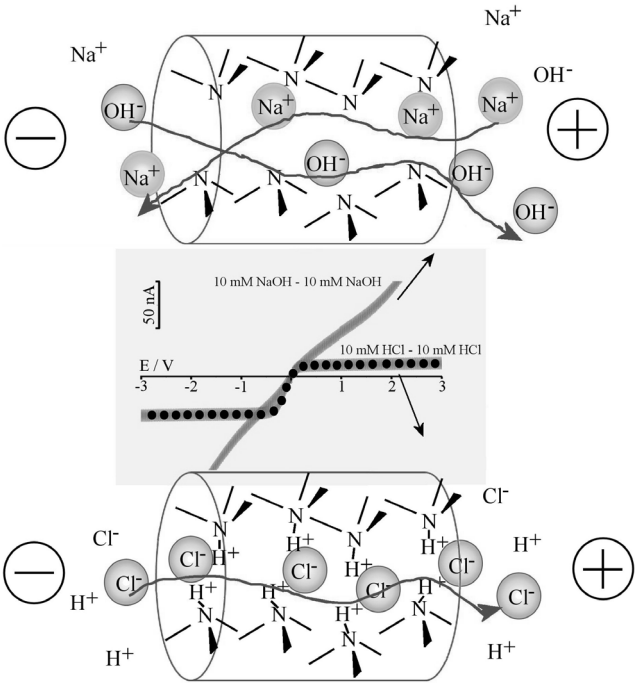

Figure 3. Experimental voltammograms (scan rate 0.02 $V s^{-1}$) in 10 mM NaOH (left)–10 mM NaOH (right) and in 10 mM HCl (left)–10 mM HCl (right). Schematic drawings are shown to illustrate the associated mechanisms.

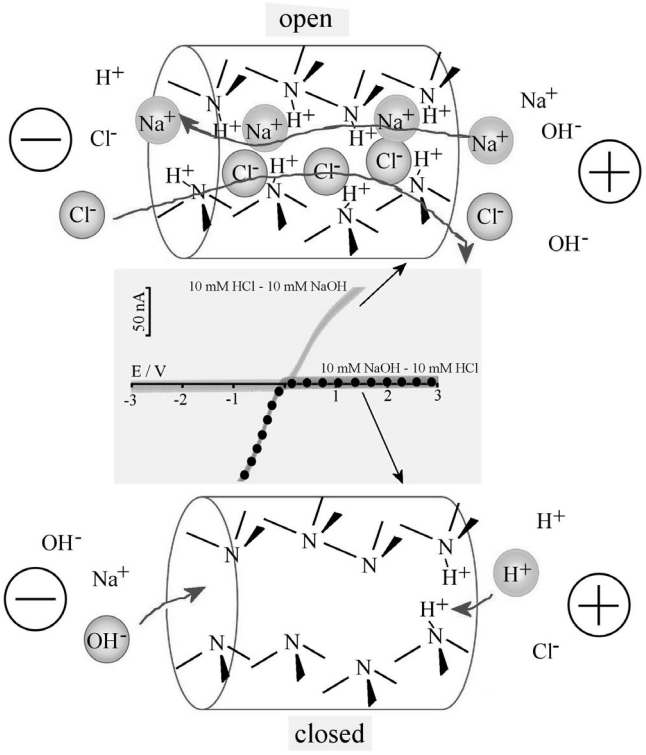

Figure 4. Experimental voltammograms (scan rate 0.02 $V s^{-1}$) in 10 mM HCl (left)–10 mM NaOH (right) and in 10 mM NaOH (left)–10 mM HCl (right). Schematic drawings are shown to illustrate the associated mechanisms.

state and complete loss of conductivity in the "closed" state (Figure 4). In the "open" state the current scales with the electrolyte concentration, but in the closed state only a high resistance is observed. Impedance measurements at +1 V vs. SCE for the "open" state suggest $R_P = 200\ M\Omega$, whereas in the "closed" state at −1 V vs. SCE the resistance is too high to measure. The latter can be explained by the formation of a neutral depletion layer due to the reaction between H^+ and OH^-. Only the current in the "open" state is concentration-dependent (see Figure SI3).

Evidence for a molecular scale depletion zone can be obtained from exploring the effects of additives into the alkaline aqueous phase. The addition of 1 mM $NaNO_3$, Na_2SO_4, or Na_3PO_4 into the 10 mM NaOH electrolyte causes only insignificant changes in ionic diode behavior. However, a larger polyphosphate anion such as phytate[28] (inositol hexaphosphate, see Figure 5) causes a significant change in behavior in the "closed" state. Figure 5 A shows a multicycle voltammogram, in which after an initial low current region (from 0.0 to 0.5 V vs. SCE) a switch to "open" occurs at 0.7 V vs. SCE. Perhaps surprisingly, the state of the ionic diode remains open until the potential is scanned into the negative potential range to "reset" the metastable diode. This effect can be employed in chronoamperometry mode (see Figure 5 B) to repeatedly switch the ionic diode employing +2 V vs. SCE to switch "on" and −2 V vs. SCE to switch "off" with read-out at 0.25 V vs. SCE. These data also reveal a time-dependence in the switching process (here 120 s for switching pulses was employed with shorter pulses less than 10 s being ineffective) and currents in the "on" state showing a drift even after 180 s. The molecular level reasons for the slow switching and the current drift are currently unknown. Initially, the large polyphosphate anions may be able to "bridge" a narrow depletion zone and so allow some limited ion flow. The "switching potential" is phytate-concentration-dependent with lower concentrations moving the switching potential to higher potentials (see Figure SI4). In the future, this phenomenon will allow the effects of molecular structure (e.g. of different types of biological polyphosphates) to be assessed and ultimately exploited in analytical devices.

It has been shown that the microporous polyamine PIM-EA-TB possesses the ability to switch from protonated anion-conducting to neutral anion/cation-conducting behavior. The suppressed proton conductivity, attributed to isolated amine sites and exceptional chain rigidity of the polymer, appears to be responsible for the generation of an ionic diode, in which a highly resistive state is switched into a highly conductive state by reversing the externally applied potential. This ionic diode is fabricated without employing complex hydrogel interfaces or nanomachining of conical nanopores. Metastable behavior can be induced into the highly resistive state of the diode, for example by phytate polyanions. Due to the direct access to well-defined PIM materials by polymer synthesis (no cross-linking, no nanofabrication) further structural variation and ion site content optimization will allow the performance of ionic diodes to be tailored toward applications as sensors and ionic current devices in membranes.

 © 2014 Wiley-VCH Verlag GmbH & Co. KGaA, Weinheim

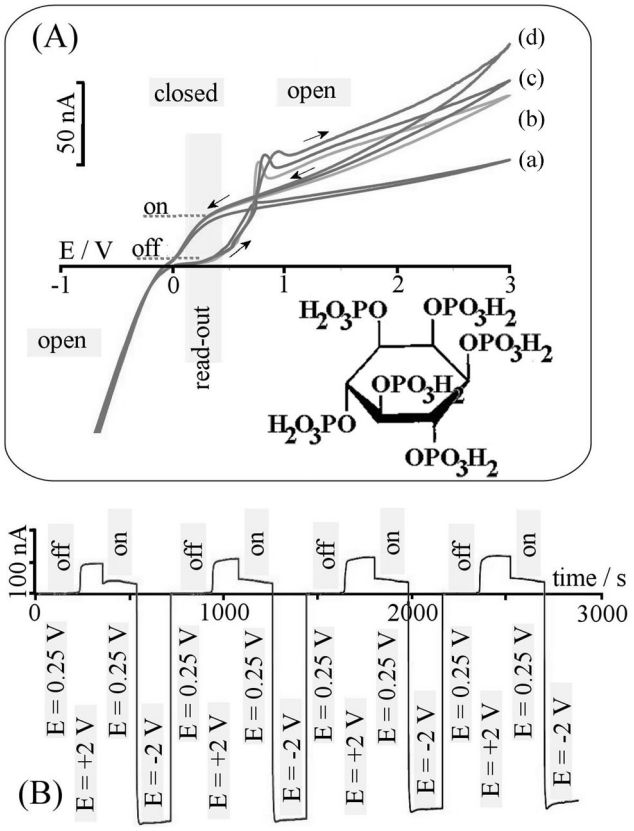

Figure 5. A) Experimental voltammograms (four consecutive cycles, scan rate 0.02 $V s^{-1}$) in 10 mM HCl (left)–10 mM NaOH (right) with 1 mM phytate added. Hysteresis and bistable switching occurs at 0.25 V vs. SCE. The molecular structure of phytic acid is shown. B) Chronoamperometry for potential-step switching and on/off behavior as a function of time.

Experimental Section

Chemical Reagents. Polymer PIM-EA-TB was prepared following a literature procedure.[13] Hydrochloric acid (30%), NaOH, chloroform, phytic acid, and phosphoric acid (85%) were obtained from Aldrich or Fisher Scientific and used without further purification. Solutions were prepared with filtered/deionized water of resistivity 18.2 MΩ cm from a Thermo Scientific water purification system (Barnstead Nanopure).

Instrumentation. An Autolab potentiostat system (PGSTAT12, EcoChemie, The Netherlands) was employed with Pt wires as counter/working electrodes, and two KCl-saturated calomel reference electrodes (SCE, Radiometer, Copenhagen). Data were recorded with GPES software.

For BET measurements (on a Quantachrome Autosorb-1), each sample was degassed under vacuum at 120 °C until the no further degassing was observed. Using Nitrogen as the adsorbate gas at 77 K, an 80 point physisorption analysis was undertaken and the data analyzed by the DFT method (N_2 at 77 K, cylindrical pore, NLDFT equilibrium model). The surface area of the samples was calculated with the BET method using a 80-point analysis.

For membrane measurements, the PIM-EA-TB polymer was dissolved into chloroform (1 $mg cm^{-3}$) by ultrasonication for 15 min and applied to a PET film with ca. 4 μm diameter holes (supplied by Laser Micromachining Limited, St. Asaph, Denbighshire LL17 0JG, UK).

Received: May 29, 2014
Revised: July 9, 2014
Published online: August 11, 2014

Keywords: diodes · fuel cells · membranes · polymers

[1] H. J. Koo, S. T. Chang, O. D. Velev, *Small* **2010**, *6*, 1393.
[2] M. Eigen, L. Demaeyer, *Z. Elektrochem.* **1955**, *59*, 986.
[3] B. Lovrecek, A. Despic, J. O. M. Bockris, *J. Phys. Chem.* **1959**, *63*, 750.
[4] L. Hegedus, Z. Noszticzius, A. Papp, A. P. Schubert, M. Wittmann, *ACH-Models Chem.* **1995**, *132*, 207.
[5] L. Hegedüs, N. Kirschner, M. Wittmann, P. Simon, Z. Noszticzius, T. Amemiya, T. Ohmori, T. Yamaguchi, *Chaos* **1999**, *9*, 283.
[6] L. Hegedus, N. Kirschner, M. Wittmann, Z. Noszticzius, *J. Phys. Chem. A* **1998**, *102*, 6491.
[7] L. Krasemann, B. Tieke, *Langmuir* **2000**, *16*, 287.
[8] J. H. Han, K. B. Kim, H. C. Kim, T. D. Chung, *Angew. Chem.* **2009**, *121*, 3888–3891; *Angew. Chem. Int. Ed.* **2009**, *48*, 3830–3833.
[9] Z. Siwy, A. Fulinski, *Phys. Rev. Lett.* **2002**, *89*, 198103.
[10] M. Ali, P. Ramirez, S. Mafe, R. Neumann, W. Ensinger, *ACS Nano* **2009**, *3*, 603.
[11] K. Zielinska, A. R. Gapeeva, O. L. Orelovich, P. Yu. Apel, *Nucl. Instrum. Methods Phys. Res. Sect. B* **2014**, *326*, 131.
[12] Y. F. Liu, L. Yobas, *Biosens. Bioelectron.* **2013**, *50*, 78.
[13] M. Carta, R. Malpass-Evans, M. Croad, Y. Rogan, J. C. Jansen, P. Bernardo, F. Bazzarelli, N. B. McKeown, *Science* **2013**, *339*, 303.
[14] P. M. Budd, B. S. Ghanem, S. Makhseed, N. B. McKeown, K. J. Msayib, C. E. Tattershall, *Chem. Commun.* **2004**, 230.
[15] N. B. McKeown, P. M. Budd, *Macromolecules* **2010**, *43*, 5163.
[16] N. B. McKeown, B. Gahnem, K. J. Msayib, P. M. Budd, C. E. Tattershall, K. Mahmood, S. Tan, D. Book, H. W. Langmi, A. Walton, *Angew. Chem.* **2006**, *118*, 1836; *Angew. Chem. Int. Ed.* **2006**, *45*, 1804.
[17] S. V. Adymkanov, Y. P. Yampol'skii, A. M. Polyakov, P. M. Budd, K. J. Reynolds, N. B. McKeown, K. J. Msayib, *Polym. Sci.* **2008**, *50*, 444.
[18] P. M. Budd, N. B. McKeown, B. S. Ghanem, K. J. Msayib, D. Fritsch, L. Starannikova, N. Belov, O. Sanfirova, Y. P. Yampol'skii, V. Shantarovich, *J. Membr. Sci.* **2008**, *325*, 851.
[19] C. G. Bezzu, M. Carta, A. Tonkins, J. J. C. P. Bernardo, F. Bazzarelli, N. B. McKeown, *Adv. Mater.* **2012**, *24*, 5930.
[20] Y. Wang, N. B. McKeown, K. J. Msayib, G. A. Turnbull, I. D. W. Samuel, *Sensors* **2011**, *11*, 2478.
[21] F. Xia, M. Pan, S. C. Mu, R. Malpass-Evans, M. Carta, N. B. McKeown, G. A. Attard, A. Brew, D. J. Morgan, F. Marken, *Electrochim. Acta* **2014**, *128*, 3.
[22] Y. Rong, R. Malpass-Evans, M. Carta, N. B. McKeown, G. A. Attard, F. Marken, *Electroanalysis* **2014**, DOI: 10.1002/elan.201400085.
[23] P. W. Atkins, *Physical Chemistry*, Oxford University Press, Oxford, **1995**, p. 834.
[24] K. B. Oldham, J. C. Myland, *Fundamentals of Electrochemical Science*, Academic Press, Toronto, **1994**, p. 285.
[25] R. Mills, V. M. M. Lobo, *Self-diffusion in Electrolyte Solutions*, Elsevier, Amsterdam, **1989**.
[26] W. Guo, Y. Tian, L. Jiang, *Acc. Chem. Res.* **2013**, *46*, 2834.
[27] G. Nguyen, I. Vlassiouk, Z. S. Siwy, *Nanotechnology* **2010**, *21*, 265301.
[28] C. Y. Cummings, A. H. Roweth, A. K. Z. Ching, A. T. A. Jenkins, J. M. Mitchels, S. Shariki, S. Y. Liew, W. Thielemans, D. A. Walsh, F. Marken, *Electrochem. Commun.* **2010**, *12*, 1722.

© 2014 Wiley-VCH Verlag GmbH & Co. KGaA, Weinheim